

DISCLAIMER

This report was prepared as an account of work sponsored by an agency of the United States Government. Neither the United States Government nor any agency thereof, nor any of their employees, makes any warranty, express or implied, or assumes any legal liability or responsibility for the accuracy, completeness, or usefulness of any information, apparatus, product, or process disclosed, or represents that its use would not infringe privately owned rights. Reference herein to any specific commercial product, process, or service by trade name, trademark, manufacturer, or otherwise does not necessarily constitute or imply its endorsement, recommendation, or favoring by the United States Government or any agency thereof. The views and opinions of authors expressed herein do not necessarily state or reflect those of the United States Government or any agency thereof.

ORNL/RSIC--48

DE87 002165

ANS/SD-86/17

Engineering Physics and Mathematics Division

**APPROXIMATE CALCULATIONAL TECHNIQUES FOR RADIATION
PROTECTION APPLICATIONS
(COLLECTION OF PAPERS PRESENTED AT THE NOVEMBER 1985
AMERICAN NUCLEAR SOCIETY MEETING)**

Sponsored by the Radiation Protection
and Shielding Division
of the American Nuclear Society

Compiled by

ALICE F. RICE

and

ROBERT W. ROUSSIN

Radiation Shielding Information Center

Published: September 1986

Prepared by the
OAK RIDGE NATIONAL LABORATORY
Oak Ridge, Tennessee 37831
operated by
MARTIN MARIETTA ENERGY SYSTEMS, INC.
for the
DEPARTMENT OF ENERGY
under contract No. DE-AC05-84OR21400

MASTER

DISTRIBUTION OF THIS DOCUMENT IS UNLIMITED

14-MEV NEUTRON STREAMING THROUGH SHIELD GAPS

W. T. Urban

Los Alamos National Laboratory

ABSTRACT Monte Carlo calculations have been performed to determine the neutron streaming through straight and single-bend gaps for three different shield thicknesses. A uniform plane source emitting 14-MeV neutrons with a cosine angular distribution was used in the analyses. The results obtained are discussed in terms of how they might be used in the early stages of a shield design to obtain approximate solutions to design questions. These results have direct implications regarding neutron-streaming problems that will be encountered in the shielding analyses of tokamak fusion reactors which are constructed from "pie-shaped" shield/vacuum chamber segments.

I. INTRODUCTION

The advance from conceptual to construction design of fusion reactors will require that shield irregularities be dealt with in detail. Many of the toroidal tokamak fusion reactor designs call for the construction of the plasma vacuum chamber and inner and outer shields through the use of "pie-shaped" segments. Figure 1 provides a schematic of a tokamak and indicates

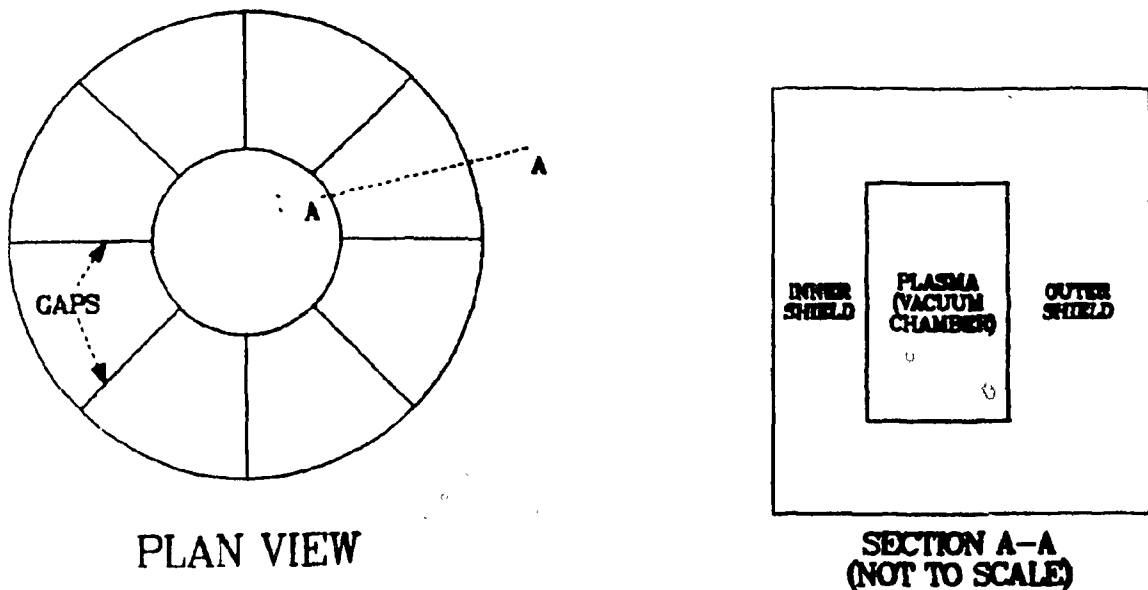


Fig. 1. Schematic of a tokamak fusion reactor in plan view and a section through the torus.

the shield/vacuum chamber segments and location of the gaps. These gaps break the continuity of the shield surrounding the vacuum chamber wherein the 14-MeV neutrons are born. Although various conceptual ideas have been suggested regarding the geometric interface between two adjacent segments, it is clear from basic shield design principles that some offsets in the gaps will probably be required together with exterior shielding at the end of the gap to reduce neutron streaming through any gap which exists between the adjacent shield segments.

A rigorous analyses of neutron streaming through shield gaps could require unacceptably expensive three-dimensional transport calculations. Thus, there is a strong incentive to use approximate techniques in the early (iterative) stages of the design process and to perform rigorous transport calculations for only the final design, if at all. Current analyses of fission reactor shield gaps and penetrations rely not only on transport calculations but also on a wide variety of semi-analytic approximate formulas which have been developed over the years on the basis of parametric studies and experimental data. Presented herein are the results of parametric studies and subsequent approximate formulas for various fusion reactor shield gap configurations based on the results of three-dimensional neutron transport calculations. This work incorporates and extends previous efforts [1,2].

II. MODEL SPECIFICATIONS AND CALCULATIONS

The "pie-shaped" segments of a torus would indicate that a curvilinear geometry might be appropriate for examining the streaming of neutrons in the gap between adjacent shield segments. However, because of the large radius of the toroid at the plasma/outer shield interface, the geometric model considered was a gap through a slab as illustrated in Fig. 2. Although many parameters have been examined, the results presented here deal primarily with variations in the shield thickness (t_s), gap width (w_g), and bend angle (θ_b).

The shield consisted of a homogeneous mixture of 80 v/o SS316 and 20 v/o water. The 0.01-m-thick canning material is SS316 and the gap is a void. The shield was two meters high and of infinite extent on either side of the gap. Shield thicknesses of 0.5, 0.75, and 1.0 meters were considered together with gap widths of 0.02, 0.05, and 0.10 meters and bend angles of 180 degrees (i.e., a straight gap), and 120 degrees. Also, for comparison, calculations were made with no gap (i.e., a solid shield), for each shield thickness.

The neutron source used was a monoenergetic (14-MeV) plane source which produced neutrons with a cosine angular distribution, that is, peaked toward the shield. This source was based on previous calculations which determined the angular dependence of 14-MeV neutrons incident on the outer shield at the outer shield/vacuum chamber interface [3]. The source plane was located 10⁻⁴ meters from the shield face and was two meters high and of infinite width.

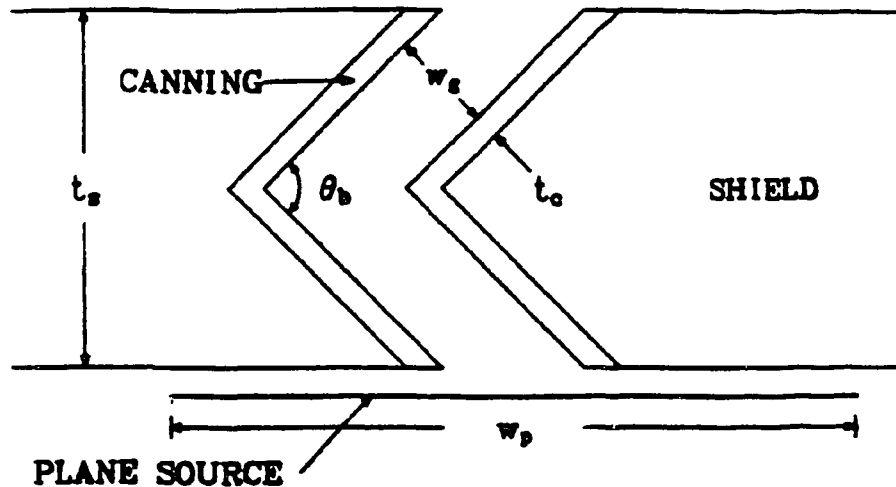


Fig. 2. Plan view illustrating the shield gap configuration (not to scale).

Calculations were made using the continuous energy Monte Carlo code MCNP [4]. Sampling of the plane source used both spatial and angular biasing. Transport of the neutrons through the gaps relied heavily on geometric splitting, Russian Roulette, and energy splitting. Cross sections were taken from a data library based on ENDF/B-IV data. Neutron dose rates were obtained through the use of the flux-to-dose conversion factors from Table G.1 of Ref. 4. The neutron dose rates reported are integral values over the energy range from 10^{-6} MeV to the source energy, 14 MeV. Point detectors and track length estimators were used in the Monte Carlo calculation of the dose rates. Point detectors were located on the centerline of the gap at the half height of the shield and at the outer edge of the shield, that is, the side of the shield opposite the source plane. Track length estimators of the flux (and thus the dose rate) within cells throughout the models were determined to provide additional confidence in the point detector results as well as to determine the dose rate falloff down the gaps. Because the calculational cells in the gap extended over the shield height, the dose rate falloff calculated along the gaps are average values, horizontally and vertically, rather than point values at the horizontal and vertical gap centerline as obtained from the point detectors. Integral dose rate values reported all have fractional errors of less than 10% with nearly all of the errors being less than 5%.

In the gap calculations, each MCNP calculation is automatically normalized to one source neutron. Hence, no additional normalization was undertaken. The average dose rates at the entrance to the gaps are in statistical agreement. The actual magnitude of the results is not of

importance; rather, it is the relative values which are important in evaluating the dose rate attenuation down the gaps and in assessing the effect of geometry changes on the dose rate attenuation.

III. RESULTS

Monte Carlo calculations were performed for variations of the configuration illustrated in Fig. 2. Variables included in these parametric calculations were the shield thickness and height; the gap width, height, bend angle, and canning thickness; and the source height and spectrum. This paper deals primarily with variations in the shield thickness, gap width and bend angle, either 180 or 120 degrees with 180 degrees corresponding to a straight gap. When a single bend gap case is considered, the bend occurs midway into the shield.

Figures 3 and 4 present the relative neutron dose rate falloff versus gap width for three different shield thicknesses. Data for the straight gap is plotted in Fig. 3 and that for the single bend gap is plotted in Fig. 4. Error bars shown in these figures are at the one-sigma confidence level. One of the most obvious observations coming from these two figures is that in

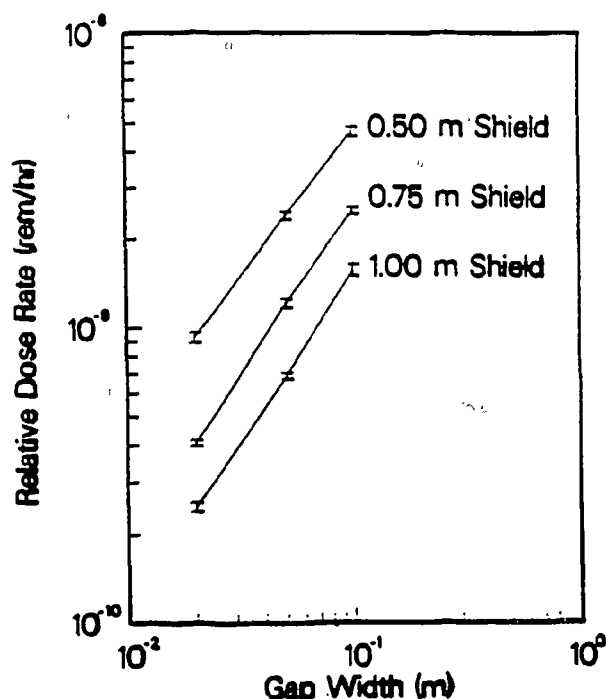


Fig. 3. Exit neutron dose rate versus gap width for various shield thicknesses with straight gap.

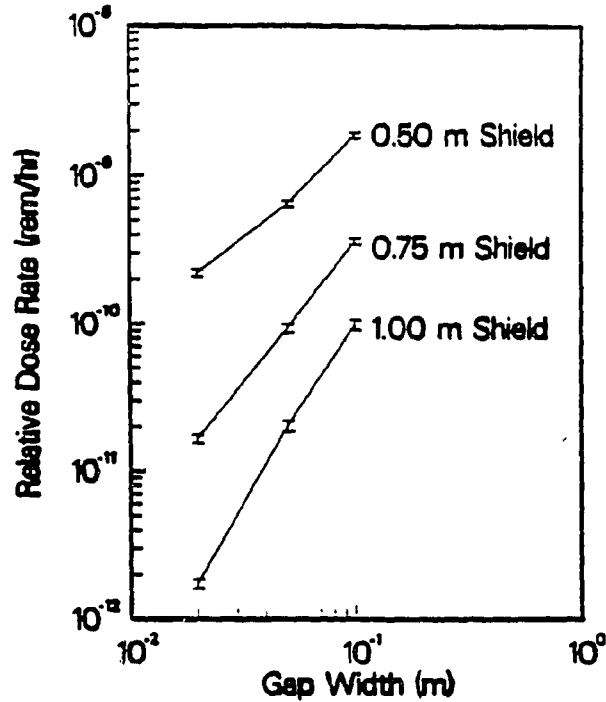


Fig. 4. Exit neutron dose rate versus gap width for various shield thicknesses with 120° gap bend angle.

both cases the relationship between the dose rate and the gap width is nearly linear when plotted using log-log scales. This suggests that the data could be fitted according to the relationship

$$\frac{D_1}{D_2} = \left(\frac{w_1}{w_2} \right)^b \quad (1)$$

where D_1 and D_2 are the exit dose rates for gap widths w_1 and w_2 , respectively, and b is a fitting parameter. A simple fit of the data yields the values of b as given in Table I for the straight and single-bend gaps for each shield thickness. Also it is observed that the falloff with the single-bend gap is approximately twice that for the straight gap. This approach is not new in that this is the same formalism that has been used for the semi-empirical neutron streaming equations developed for the analyses of fission reactor shield gaps [5].

Similarly the data of Figs. 3 and 4 can be replotted with neutron dose rate versus shield thickness for three different gap widths to obtain Figs. 5 and 6. Again the linearity of the data when plotted on log-log paper is apparent, suggesting this data could be fit according to

$$\frac{D_1}{D_2} = \left(\frac{t_1}{t_2} \right)^c \quad (2)$$

TABLE I

Dose Rate versus Gap Width Fitting Parameter b^*

Shield Thickness (m)	Fitting Parameter b	
	Straight Gaps	Single Bend Gaps
0.50	1.00	1.32
0.75	1.13	1.91
1.00	1.15	2.51

*See Equation (1).

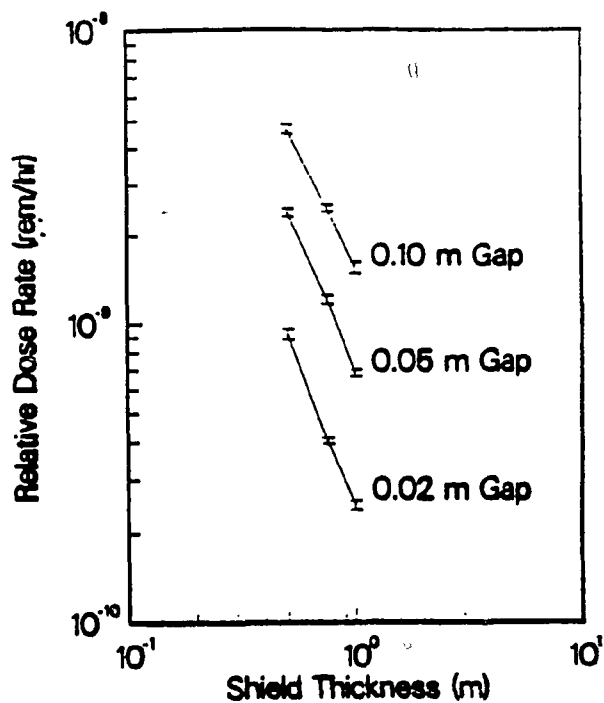


Fig. 5. Exit neutron dose rate versus shield thickness for straight gaps.

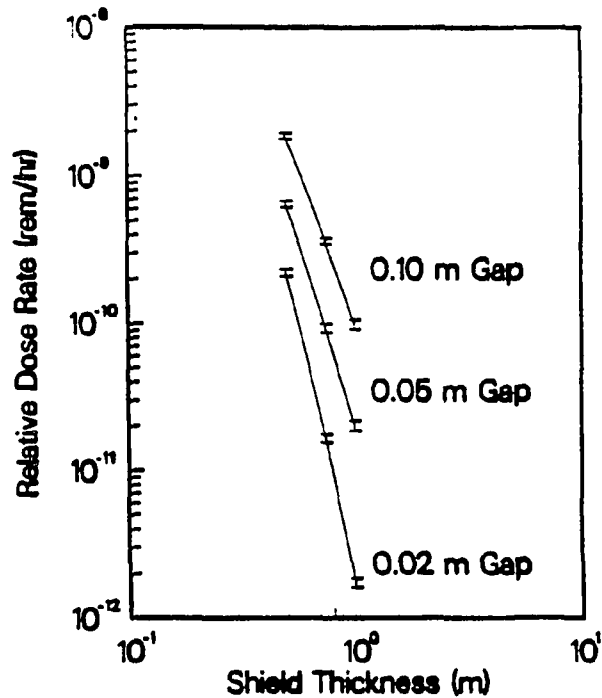


Fig. 6. Exit neutron dose rate versus shield thickness for single-bend gaps of 120° .

where D_1 and D_2 are the exit dose rates for shield thicknesses t_1 and t_2 , respectively, and c is the fitting parameter. Values for the parameter c for each gap width are provided in Table II.

TABLE II

Dose Rate versus Shield Thickness Fitting Parameter c^*

Gap Width (m)	Fitting Parameter c	
	Straight Gaps	Single Bend Gaps
0.10	-1.57	-4.23
0.05	-1.81	-4.98
0.02	-1.91	-6.99

*See Equation (2).

Although the data provided in Figs. 3-6 is certainly helpful, the shield designer should also be interested in the dose rate falloff as a function of distance from the source. This information is provided in a variety of ways in Figs. 7 through 10 for straight and single-bend gaps in a 0.75-meter-thick shield. For comparison the dose rate falloff through the solid, that is, no gap, shield is also plotted. These neutron dose rates are cell-averaged values and the cells extend over the height of the gap. Also recall that the source plane is only 10^{-4} m from the shield face. Several observations are worth noting regarding this data.

From Fig. 7 it is seen that even a very small straight gap significantly increases the dose rate, but as the gap width increases, the dose rate also increases in apparently direct proportion to the gap width increase. Also, it can be seen that for the no gap case, the falloff is nearly exponential, that is, a straight line on a semilog plot, whereas for the three straight gap cases it is not an exponential falloff. In each of the gap cases the initial falloff appears to be exponential and then appears to fall off more slowly with distance from the source. This effect becomes more pronounced as the gap width increases. Because of this "end effect" a designer can get into trouble by trying to extrapolate the results for a gap in one shield thickness to an identical gap in a shield of a different thickness unless the "end effect" is also scaled. It should also be noted that for the solid shield there appears to be no noticeable "end effect."

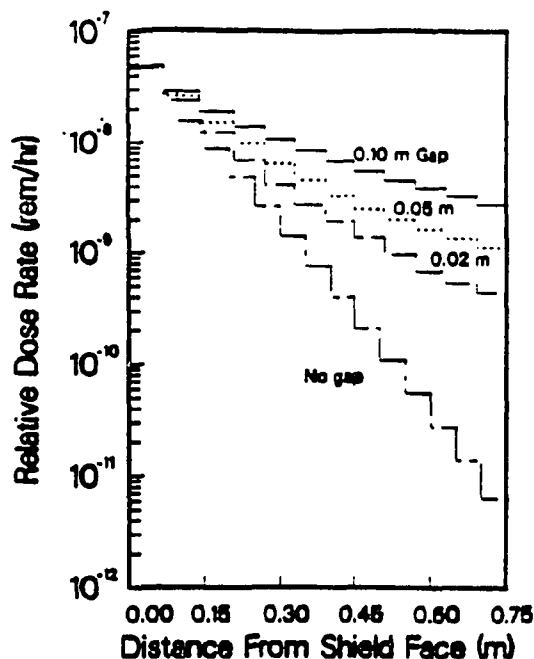


Fig. 7. Neutron dose rates in straight gaps versus distance from the shield face.

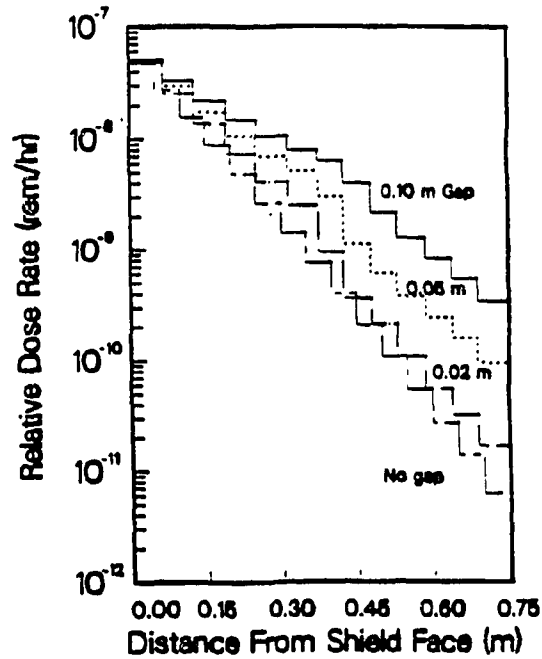


Fig. 8. Neutron dose rates in single-bend gaps versus distance from the shield face.

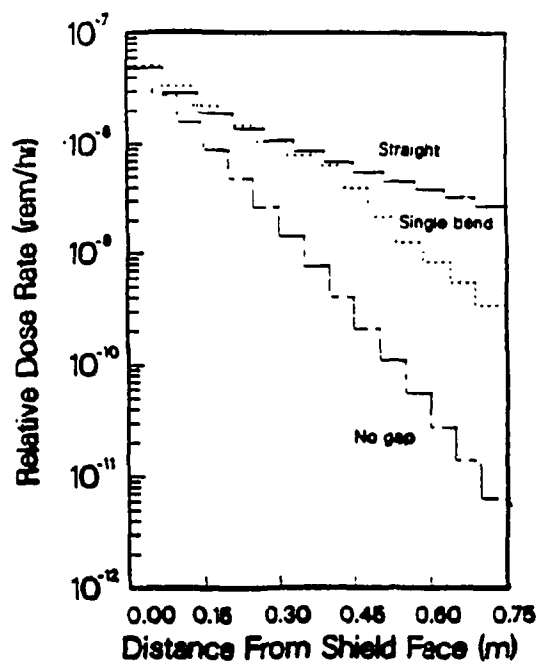


Fig. 9. Neutron dose rates in 0.10 m straight and single-bend gaps in a 0.75 shield versus distance from the shield face.

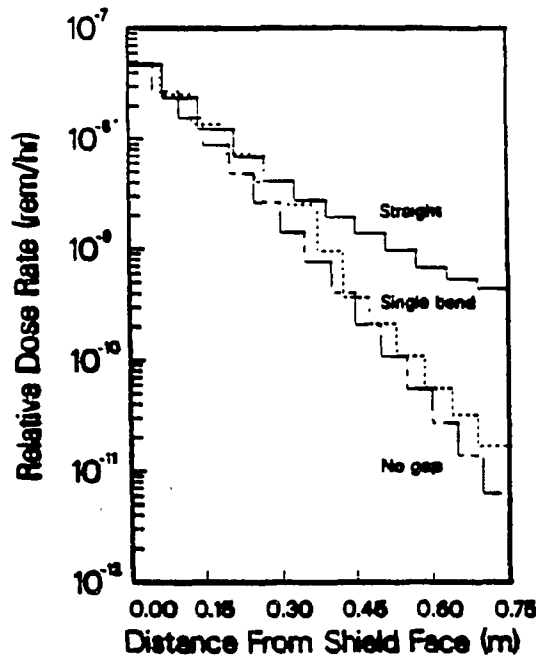


Fig. 10. Neutron dose rates in 0.02 m straight and single-bend gaps in a 0.75 m shield versus distance from the shield face.

When the single-bend gap cases are examined in Fig. 8, several differences are immediately obvious. First it can be seen that the single-bend gap is much better than the straight gap in attenuating the neutron dose rate. Furthermore, there is essentially a hump in each of the three curves corresponding to the middle of the shield, that is, where the bend takes place. It is believed that this is due in part to backscattering at the bend which retards the attenuation in the gap just prior to the bend. In each of the two legs of the gap, the attenuation appears to be exponential, that is, linear falloff when plotted on semilog paper as in Fig. 8, but with different slopes for each leg. In the second leg the falloff is much more rapid than in the first leg.

Figures 9 and 10 illustrate the benefit obtained through the use of a midshield single bend in the gap for 0.1- and 0.02-m gaps, respectively. As expected, there is no benefit in the first leg of the gap but a substantial benefit in the second leg with the benefit increasing with decreasing gap width. Also, these two figures clearly show how the benefit of the single-bend gap over the straight gap increases with decreasing gap width.

Another quantity that is often very helpful in identifying potential shielding problems is the peaking factor. The peaking factor is simply the ratio of the dose rate at the point where the gap exits the shield to the dose rate if the gap were not present. The peaking factor data presented is based on the point detector dose rates at the geometric center of the gap on the outer edge of the shield.

Figures 11 and 12 provide the dose rate peaking factor as a function of gap width for the straight and single-bend gaps, respectively. The curves are all nearly linear on these log-log plots. Plots such as this provide a designer with an immediate estimate of the consequences of gaps in a bulk shield and help him to decide if additional shielding will be needed because of the gaps. However, in order to provide a design to shield the streaming neutrons, for example, shield battens, etc., it is necessary to have an estimate of the neutron spectrum exiting the gap. Figure 13 provides, for straight gaps, a crude estimate of the spectrum in the form of a dose rate ratio, that is, the ratio of the dose rate due to all neutrons to the dose rate due to uncollided, that is, source energy, neutrons. Although the plotted data does not seem to be linear, if one considers the expanded scale of the ordinate and the statistics of the data, then a straight line fit approach is probably not too bad. This curve also indicates that one could simply calculate an uncollided dose rate based on ray theory (point kernel approach) and then multiply it by the appropriate dose rate ratio. This technique is inappropriate for the single-bend gap, however, as a minimum of one collision is required for a neutron to traverse the shield via the gap.

What is really needed by the designer is the energy spectrum of the neutrons exiting the gap. Figure 14 contains dose rate spectrum information through a plot of fractional dose rate versus neutron energy for both

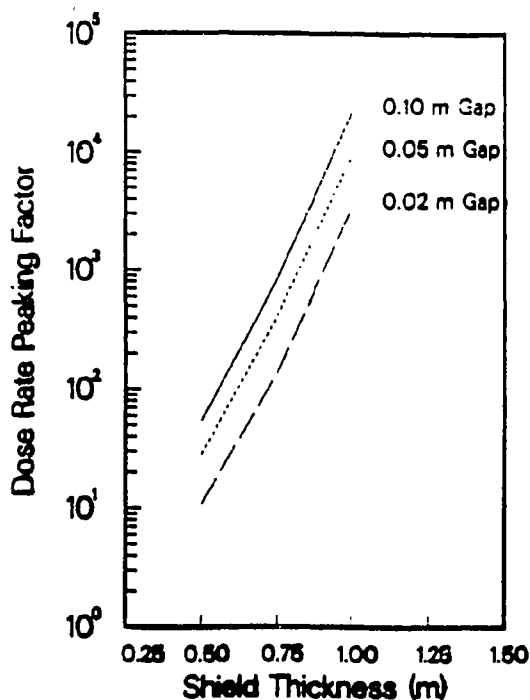


Fig. 11. Straight gap dose rate peaking factor versus shield thickness.

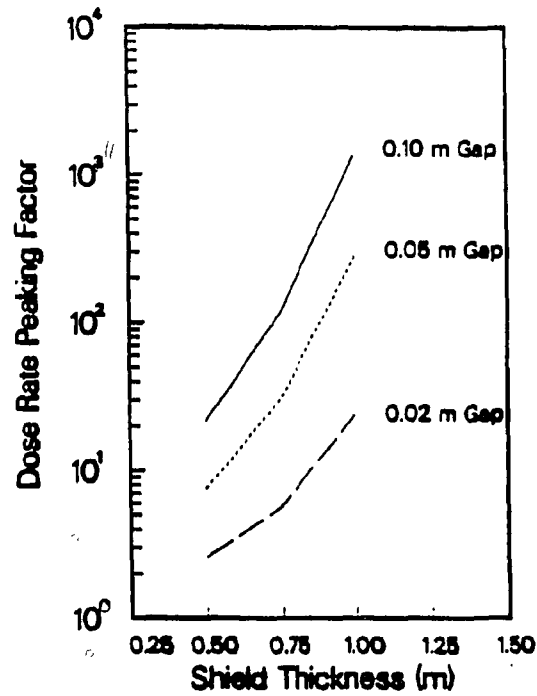


Fig. 12. Single-bend gap dose rate peaking factor versus shield thickness.

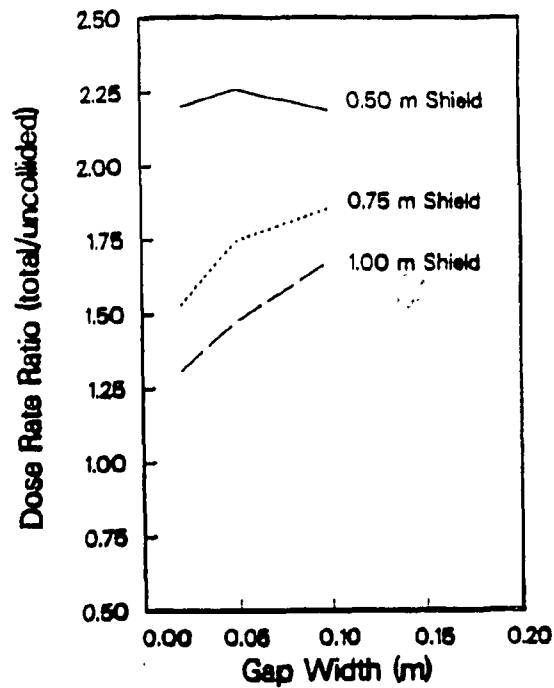


Fig. 13. Ratio of the total dose rate to the dose rate due to uncollided source neutrons versus the width of straight gaps.

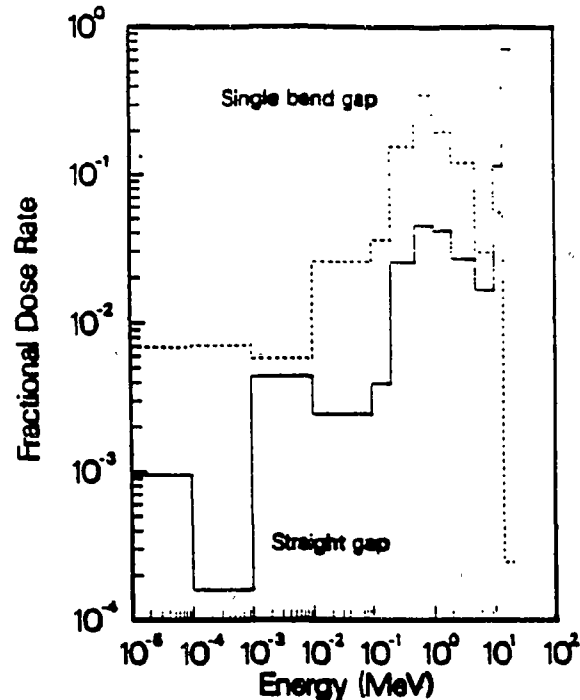


Fig. 14. Fractional dose rates versus neutron energy for 0.05 m straight and single-bend gaps in a 0.75 m shield.

straight and single-bend, 0.05-m-wide gaps in a 0.75-m-thick shield. The area under both curves is unity. Uncollided neutrons can be seen to be responsible for contributing approximately 75% of the dose rate for the straight gap. On the other hand for the single-bend gap the uncollided contribution is negligible and the majority (83%) of the dose rate comes from neutrons with energies between 0.2 and 5.0 MeV.

IV. CONCLUSIONS

Parametric studies have been performed to provide information that can be used to determine, directly or through interpolation, the dose rate for neutrons exiting various shield gap configurations. The shielding benefit of a single-bend gap over a straight gap is clearly shown. Furthermore, families of curves for both straight and single-bend gaps through shields of varying thicknesses illustrate the well-defined nature of exit-dose rate versus both shield thickness and gap width. Also, it is demonstrated that this data can be fit using the same functional form as has been used in fission reactor shield gap analyses.

ACKNOWLEDGMENTS

The author wishes to acknowledge the many helpful discussions and the support provided by Dr. Donald J. Dudziak of Los Alamos National Laboratory during the early stages of this effort. This work was supported by the U.S. Department of Energy.

REFERENCES

- [1] W. T. Urban, Neutron Streaming Through Straight and Single Bend Slots, LA-9761-MS, Los Alamos National Laboratory (July 1983).
- [2] W. T. Urban and Donald J. Dudziak, "Fusion Neutron Streaming in Shield Gaps," Trans. Am. Nucl. Soc., 50, 453 (November 1985).
- [3] W. T. Urban, T. J. Seed, and Donald J. Dudziak, "Engineering Test Facility Vacuum Pumping Duct Shield Analysis," Nucl. Tech./Fusion, 2, 261-271 (April 1982).
- [4] Los Alamos Monte Carlo Group, MCNP - A General Monte Carlo Code for Neutron and Photon Transport, Version 2B, LA-7396-M, revised, Los Alamos National Laboratory (February 1981).
- [5] Theodore Rockwell III, Ed., Reactor Shielding Design Manual, D. Van Nostrand Co., Princeton, New Jersey (1956).